

AD-A063 617

GENERAL SENSORS INC FORT WASHINGTON PA  
STUDY OF THE FEASIBILITY OF USING AN ADVANCED OPTO-ELECTRONIC I--ETC(U)  
NOV 78 H SADJIAN  
GS-ONR-2-1978

F/G 17/8

N00014-78-C-0253

NL

UNCLASSIFIED

| OF |  
AD  
A063617



END  
DATE  
FILED  
3-79  
DDC

Report GS-ONR-2-1978

GENERAL

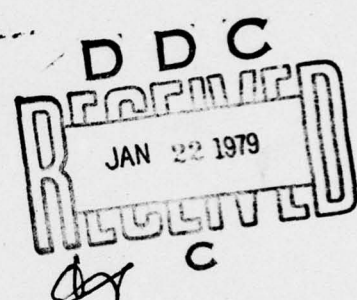


SENSORS, INC.

STUDY OF THE FEASIBILITY OF USING AN ADVANCED OPTO-ELECTRONIC  
IMAGING TECHNIQUE FOR SAMPLING MID-WATER NEKTON

Parameters That Govern Image Quality And Pattern Recognition  
Techniques For Underwater Optical Imaging

LEVEL



DDC FILE COPY, ADA063617

Harry Sadjian  
GENERAL SENSORS, INC.  
500 Office Center Drive  
Ft. Washington, Pa. 19034

30 November 1978

Annual Report for Period 15 June 1978 - 30 September 1978

Approved for public release; distribution unlimited

Prepared for  
U. S. GEOLOGICAL SURVEY  
620 National Center  
Reston, Virginia 22092

OFFICE OF NAVAL RESEARCH  
800 N. Quincy Street  
Arlington, Virginia 22217

79 01 16 072 Copy No. 33....

(14) Report GS-ONR-2-1978

(P)

(6) STUDY OF THE FEASIBILITY OF USING AN ADVANCED OPTO-ELECTRONIC  
IMAGING TECHNIQUE FOR SAMPLING MID-WATER NEKTON

Parameters That Govern Image Quality And Pattern Recognition  
Techniques For Underwater Optical Imaging

(10) Harry Sadjian  
GENERAL SENSORS, INC.  
500 Office Center Drive  
Ft. Washington, Pa. 19034

DDC  
DRAFTED JAN 22 1979  
UNCLASSIFIED

(11) 30 November 1978

(12) 43p.

(9) Annual Report for Period 15 June 1978 - 30 September 1978

Approved for public release; distribution unlimited

Prepared for  
U. S. GEOLOGICAL SURVEY  
620 National Center  
Reston, Virginia 22092

(15) N 40014-78-C-0253

OFFICE OF NAVAL RESEARCH  
800 N. Quincy Street  
Arlington, Virginia 22217

410 437

79 01 16 082

JOB

UNCLASSIFIED

SECURITY CLASSIFICATION OF THIS PAGE (When Data Entered)

DD FORM 1 JAN 73 1473

**EDITION OF 1 NOV 68 IS OBSOLETE  
S/N 0102-014-6601 |**

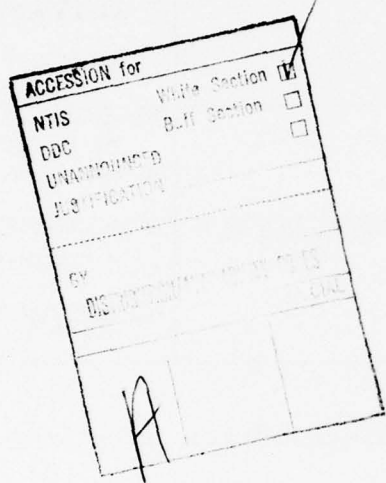
UNCLASSIFIED  
SECURITY CLASSIFICATION

UNCLASSIFIED

SECURITY CLASSIFICATION OF THIS PAGE(When Data Entered)

20. ABSTRACT (cont'd)

in offshore oil drilling.



UNCLASSIFIED

SECURITY CLASSIFICATION OF THIS PAGE(When Data Entered)

30 November 1978

STUDY OF THE FEASIBILITY OF USING AN ADVANCED OPTO-ELECTRONIC  
IMAGING TECHNIQUE FOR SAMPLING MID-WATER NEKTON

Parameters That Govern Image Quality And Pattern Recognition  
Techniques For Underwater Optical Viewing

The objective of this program is to determine the applicability of pattern recognition techniques for underwater optical imaging in turbid coastal waters. In conjunction with the Survey's untethered, unmanned underwater inspection vehicle study, this study is being conducted as an adjunct to an acoustic control and link to the surface. Preparatory to investigating pattern recognition techniques, this phase of the study has addressed the problem of the resulting image quality to be expected in turbid waters and the degree of recovery from a detector system. Starting from the basic equation for incoherent imaging, the point source response for seawater is derived incorporating the attenuation and scattering coefficients of seawater with a general expression derived for the scattering function. Equations are presented that indicate how scattering background, type of object, reflectivity, type of illumination and related parameters are incorporated into the imaging equations. Working in the Fourier frequency domain, equations are derived that relate the degradation of image quality to shot noise, electronic noise and to the type and mode of scanning of the detector system. A flow diagram is developed that shows how the various variables are related to the final image quality. Recommendations are made as to the course of the future study. This work was performed for the U. S. Geological Survey and was administered by the Office of Naval Research.

GS-ONR-2-1978

30 November 1978

We are pleased to acknowledge the encouragement and guidance provided by Mr. John Gregory, Research Program Manager of the OCS Operations at the U. S. Geological Survey during the course of this study. We also express our sincere gratitude to Dr. E. Silva of ONR in Arlington, Virginia for allowing this program to be administered through ONR.

TABLE OF CONTENTS

ABSTRACT .....	v
ACKNOWLEDGEMENTS .....	vi
I. INTRODUCTION .....	1
II. DERIVATION OF SEAWATER TRANSFER FUNCTION .....	5
A. Background .....	5
B. Theory .....	6
1. Derivation of the Point Spread Function ....	7
2. Derivation of the $\tilde{C}_{sw}$ .....	11
3. Determination of the Transform of $\sigma(\theta)$ ...	12
III. EVALUATION OF DETECTOR RESPONSE .....	19
IV. EFFECT OF DETECTOR SCANNING .....	27
V. SUMMARY AND RECOMMENDATIONS .....	31
References .....	33
Figures .....	35

## I INTRODUCTION

In conjunction with the U. S. Geological Survey's untethered, unmanned underwater inspection vehicle study, pattern recognition technology is being investigated as an adjunct to an acoustic control and data link to the surface. Pattern recognition is terminology for grouping observations so that only the desired data is retrieved for analysis. Such grouping is desirable primarily to hasten the retrieval of wanted data and to avoid storing and analysing unwanted data. The recognition of patterns of data can be applied to optical or acoustical imaging or even to physical measurements.

The primary means of inspection used by present day submersibles is visual and photography. Optical imaging is therefore an obvious starting point for recognition studies. However, whereas the Navy is studying optical imaging for the mid-waters of the ocean, where turbidity or water clarity is not a major factor, offshore structures are located around the coastline of the United States in relatively shallow waters which have great turbidity variance. In order to be able to perform remote optical surveillance of underwater offshore oil drilling structures and associated oil pipelines, it is necessary, as a first step, to examine the expected quality of the image received by an active (i.e. artificially illuminated) untethered robot viewing system.

For a robot viewing system that is acoustically interrogated and controlled, the amount of information that can be transmitted by normal imaging techniques (e.g. TV, etc.) will be severely limited due to the limitation in the data rate of an acoustic data link. Consequently, it becomes desirable to consider the incorporation of a degree of "intelligence" in the robot vehicle in order to reduce

the amount of data that must be transmitted by the acoustic link to the surface.

For high quality imagery, where the intervening medium does not distort the image, existing computer assisted techniques are available to extract key features of the image (rejecting undesired image features) for analysis by preprogrammed computer to determine and transmit the desired information.

As the offshore oil drilling structures will be operating at various depths (few hundred to a few thousand feet), the variability of the ocean imaging characteristics becomes paramount. In addition to the variability of the water clarity which distorts the image received by the robot viewing system, the available illumination, the type of object viewed, the type of detector used all contribute to the final image received. As the final image will vary in clarity, the ability of a recognition computer to perform the necessary analysis before transmission to the surface will also depend on this image clarity. Consequently, the performance of a remote surveillance system will depend on the ability of the "intelligence" built into the system to compensate for this changing image quality.

This present work has examined the various factors that determine the image quality in order to subsequently determine the feasibility of incorporating the requisite "intelligence" into the viewing robot vehicle. In figure 1, we have depicted in flow diagram form the variables that go into the formation of the final image as received by the robot vehicle. The legend on the left of the figure indicates those parameters that this current work has addressed.

The most important parameter (box 5, figure 1) is the imaging characteristics of the sea water. As a result of this work, we have been able to characterize it in terms of three well defined variables.

These are  $\alpha$ , the attenuation coefficient;  $s$ , the scattering coefficient in the forward direction;  $N$ , the log-log slope of the scattering function. This method of characterization has been developed during the course of this study and represents a departure from the conventional characterization of the sea-water optical properties (see section II below). The other variables have been treated in a conventional manner except that in the final image (box 12, figure 1), the result is expressed in spatial frequency terms rather than image resolution terms. The motivation for this method of characterization of the final image stems from the ability to treat imaging systems as linear filters of spatial frequencies (i.e. reciprocal of resolution element). This is exactly analogous to treating electrical waveforms as a mixture of temporal frequencies except in the optical case it is two dimensional. This method of image characterization (Fourier Analysis) simplifies the image analysis immeasurably by obviating the necessity of solving the more difficult diffraction integrals used for describing the resultant image.

In the following sections, each box of figure 1 is addressed separately except box 13. This will require the expected scenario and optical configuration to be used for viewing before the pattern recognition hierarchy can be evolved.

In section II, we treat the most difficult variable, the characterization of the optical properties of the sea-water in terms of the three simple parameters mentioned above. In sections III and IV, we examine the degradation that may be caused by the type of detector used and the mode of recording. A summary is presented in section V of the results of this analysis and the necessary steps to be taken in future work before the feasibility of using a pattern recognition technique for underwater surveillance can be evaluated.

## II DERIVATION OF SEAWATER TRANSFER FUNCTION

As indicated in the introduction, the characterization of the sea-water optical properties is the most difficult variable to quantify. One approach has been to formulate an expression for the spread function ( angular distribution of intensity with distance) for a collimated or focused beam in sea-water. In general no closed closed form expressions has been found except for short ranges which involves the integration of the volume scattering function. It has been found by Wells<sup>(1)</sup> that the optical properties of the sea-water can be expressed more easily by working in the Fourier Domain (i.e. working with the Fourier transform of the spread function). However, as explained below, we have modified this method of expression so that experimentally derived scattering function can be used directly. This modified method allows the use of the many measurements that have been made for a number of years to be used without resorting to a mathematical model for the scattering function.

### A. Background:

Originally, we had intended to use the closed expressions derived by Wells for the sea-water transfer function in conjunction with the experimentally derived scattering functions by the Scripps Institute of Oceanography<sup>(2)</sup> off the coast of Southern California.

We have found that the experimental data does not correlate well with the mathematical model for the scattering function given by Wells. It became apparent that in order to assess the image quality in turbid waters, it would be necessary to modify the Wells theory in order to utilize the experimental data directly without the use of a mathematical model for the scattering function. We have attempted to formulate the modification using simple parameters resulting in the development

of the imaging equations from the first principles of Fourier Optical Theory. As a result of the additional time that was necessary to develop the imaging equations from ground zero, so to speak, we are not as far along as originally planned. However, the equations that have been developed have general application and only require the experimentally derived scattering function, for a given type of ocean, detector characteristics and object structure to assess the image quality.

#### B. Theory:

The underlying equation that governs imaging in incoherent light is given by,

$$I(x,y) = \iint O(\xi,\eta) S(x-\xi, y-\eta) d\xi d\eta \quad (1)$$

where,

$I(x,y)$  = resultant image intensity distribution in the image plane

$O(\xi,\eta)$  = object intensity distribution in the object plane

$S(x,y)$  = response of the system(seawater plus optics) to a point source-- the point spread function

and where the integral represents a convolution of the object distribution with the point spread function. Equation (1) can be evaluated more readily by mathematically transforming to the spatial frequency plane by direct Fourier transformation resulting in,

$$\tilde{I}(\omega_x, \omega_y) = \tilde{O}(\omega_\xi, \omega_\eta) \cdot \tilde{S}(\omega_x, \omega_y) \quad (2)$$

where  $\tilde{\tau}$  is the optical transfer function and the  $\sim$  represents the Fourier transform of each distribution. The  $\omega$ 's represent the conjugate variables to the coordinates, termed the spatial frequency with units of radians per unit length. As can be seen, direct multiplication is less difficult to evaluate than the convolution integral of equation (1). In addition, the spatial frequency representation is a more meaningful criterion to use when evaluating resolution requirements.

In underwater viewing, it is more convenient to cast the equations in terms of angular coordinates. Consequently, equation (1) reads,

$$I(\theta_x, \theta_y) = \iint_{\text{object}} O(\theta_x, \theta_y) s(\theta_x - \theta_x, \theta_y - \theta_y) d\theta_x d\theta_y \quad (3)$$

where the  $\theta$ 's are the coordinates divided by the range on the object side and by the focal length on the image side. For example, the  $\theta_x$  would be equal to  $x/F$ . In addition, the intensities are now expressed as energy or power/steradian. Similarly, equation (2) becomes,

$$\tilde{I}(\omega_{\theta_x}, \omega_{\theta_y}) = \tilde{O}(\omega_{\theta_x}, \omega_{\theta_y}) \cdot \tilde{\tau}(\omega_{\theta_x}, \omega_{\theta_y}) \quad (4)$$

where the  $\omega$ 's are given in terms of radians(frequency)/radians(angle).

#### 1. Derivation of the Point Spread Function

In order to make the problem of deriving the point spread function in seawater tractable, we reverse the order of equation (3) and con-

sider what happens when a point source in the image plane is projected onto the object plane. The geometry is depicted in Figure 2. Consider an element of area  $dA$  in the  $x,y$  plane,  $dxdy$ . In angular coordinates,  $dA$  is  $d\theta_x d\theta_y F^2$ . A radiating surface in the  $x,y$  plane can be written as  $n_o \rho(\theta_x, \theta_y)$  where  $n_o$  is the energy/power density radiating from the surface and  $\rho(\theta_x, \theta_y)$  is the diffuse reflectivity of the surface at the coordinates  $\theta_x, \theta_y$ . The brightness of the surface becomes  $\frac{n_o \rho(\theta_x, \theta_y)}{\pi}$  assuming a Lambertian surface. Consequently, the amount of energy emanating from the elemental area is,

$$\frac{n_o \rho(\theta_x, \theta_y)}{\pi} \cdot d\theta_x d\theta_y F^2 \quad (5)$$

The lens receives  $\pi D^2 / 4F^2$  of the energy where  $D$  is the diameter of the lens. Hence the energy received by the lens is,

$$E_L = \frac{\pi D^2}{4 F^2} \cdot \frac{n_o \rho(\theta_x, \theta_y)}{\pi} \cdot d\theta_x d\theta_y F^2 \quad (6)$$

or,

$$E_L = \frac{D^2 n_o \rho(\theta_x, \theta_y)}{4} d\theta_x d\theta_y \quad (6a)$$

Now consider a single ray along the axis of the lens, represented by  $E_L dv dw / A_L$  ( $A_L$ , the area of the lens), to be propagating toward the  $\epsilon, \eta$  plane. Experimentally, a narrow collimated beam traversing a

length  $\Delta$  in water scatters according to  $\sigma(\theta)$ , the volume scattering function. Here the  $\Delta$  is assumed to be small enough that only single scattering occurs. At the end of the path length  $\Delta$ , the angular distribution for the single ray is  $\sigma(\theta)\Delta(1-\alpha\Delta)$  where the  $\alpha$  is the seawater attenuation coefficient. At the end of the second  $\Delta$ , we can consider the resultant distribution to be a convolution of the angular distribution at the end of one  $\Delta$  with itself, i.e.,

$$\sigma(\theta)\Delta(1-\alpha\Delta) \odot \sigma(\theta)\Delta(1-\alpha\Delta) \quad (7)$$

where the symbol  $\odot$  means convolution. In this derivation, as experimentally derived, the  $\sigma(\theta)$  has cylindrical symmetry and hence a function of  $\theta$  only. Continuing in this fashion until the range  $R$  is reached we have that,

$$S(\theta) = (1-\alpha\Delta)^{R/\Delta} \sigma(\theta)\Delta \odot \sigma(\theta)\Delta \dots \quad (8)$$

where the ... means that the convolution continues  $R/\Delta$  times. As the energy of the ray was  $E_L dv dw / A_L$ , we have that,

$$I_R(\theta) = \frac{E_L S(\theta) dv dw}{A_L} \quad (9)$$

where  $I_R$  is the intensity distribution of the ray at the range  $R$ . All the other rays, since without aberration of the seawater would converge at the same point, would produce the same distribution in the  $\epsilon, \eta$  plane as the axial ray. Neglecting the slight cosine dependence, the resultant distribution is the superposition of all the rays and hence,

$$I(\theta) = E_L S(\theta)$$

(9a)

Consequently an intensity distribution in the  $x, y$  plane would produce in the  $\epsilon, \eta$  plane the distribution given by,

$$I(\theta_x, \theta_y) = \frac{D^2 n_0}{4} \iint \rho(\theta_x, \theta_y) S(\theta_x - \theta_\epsilon, \theta_y - \theta_\eta) d\theta_x d\theta_y \quad (10)$$

Due to the reversibility of the light rays, we can rewrite (10) as,

$$I(\theta_x, \theta_y) = \frac{D^2 n_0}{4} \iint \rho(\theta_x, \theta_y) S(\theta_x - \theta_\epsilon, \theta_y - \theta_\eta) d\theta_\epsilon d\theta_\eta \quad (11)$$

Transforming (11), we have that,

$$I(\omega_{\theta_x}, \omega_{\theta_y}) = \frac{D^2 n_0}{4} \widetilde{\rho}(\theta_\epsilon, \theta_\eta) \cdot \widetilde{C}_{sw}(\omega_{\theta_x}, \omega_{\theta_y}) \quad (12)$$

where the  $\tilde{\mathcal{C}}_{sw}$  is the transform for the seawater.

## 2. Derivation of the $\tilde{\mathcal{C}}_{sw}$

From equation (8) and the relationship between the  $\tilde{\mathcal{C}}_{sw}$  and the  $s(\theta)$  we have that,

$$\tilde{\mathcal{C}}(\omega_\theta) = F \left\{ (1 - \alpha \Delta)^{R/\Delta} s(\theta) \Delta \odot s(\theta) \Delta \dots \right\} \quad (13)$$

where  $F \left\{ \quad \right\}$  means the Fourier transform of. From the convolution theorem we can rewrite (13) as,

$$\tilde{\mathcal{C}}(\omega_\theta) = (1 - \alpha \Delta)^{R/\Delta} \widetilde{(s(\theta) \Delta)}^{R/\Delta} \quad (14)$$

To evaluate (14), we use the basic definition for the numerical constant  $e$ , i.e.,

$$e = \lim_{\epsilon \rightarrow \infty} (1 + \epsilon)^{1/\epsilon} \quad (15)$$

With  $\epsilon = -\alpha \Delta$  for the first factor in (14) and  $\epsilon = \widetilde{s(\theta)} \Delta - 1$  for the second factor, we have that,

$$\tilde{\mathcal{C}}(\omega_\theta) = \lim_{\epsilon \rightarrow \infty} (1 + \epsilon)^{\frac{1}{\epsilon}(-\alpha R)} \cdot (1 + \epsilon)^{\frac{1}{\epsilon+1} \cdot \widetilde{s(\theta)} R} \quad (16)$$

or,

$$\tilde{\chi}(\omega_\theta) = e^{-\alpha R} \cdot e^{\tilde{\sigma}(\theta) R} \quad (17)$$

Consequently, the determination of  $\tilde{\chi}$  comes down to the determination of the transform of  $\sigma(\theta)$ .

### 3. Determination of the Transform of $\sigma(\theta)$

In order to determine the transform of  $\sigma(\theta)$ , we usually must assume some form of the scattering function. However, the experimental data indicates that the scattering function follows a log-log relationship with arbitrary slope out to at least  $1^\circ$ . Consequently, we can write that,

$$\sigma(\theta) = K \theta^{-N} \quad (18)$$

where  $K = \text{constant}$

$N = \text{arbitrary slope}$

Equation (18) indicates a singularity at  $\theta = 0$ . As experimentally the function cannot be measured at angles much less than  $.1^\circ$ , we assume that the log-log relationship holds even when  $\theta$  is less than  $.1^\circ$ . Although (18) diverges at  $\theta = 0$ , its' integral is finite as will be shown below. Consequently, (18) can be used to determine the transform directly.

Due to the cylindrical symmetry of  $\sigma(\theta)$ , the two demensional transform can be written as a one- dimensional Fourier-Bessel transform,

$$\tilde{\sigma}(\theta) = 2\pi K \int_0^\epsilon \theta^{-N} J_0(\omega\theta) \theta d\theta \quad (19)$$

where,  $J_0$  = Bessel function of zero order

$\epsilon$  = limiting angle of integration (about  $1^{\circ}$ ).

Equation (19) then becomes,

$$\tilde{\sigma}(\theta) = 2\pi K \int_0^\epsilon \theta^{1-N} J_0(\omega\theta) d\theta \quad (20)$$

with the restriction that  $N$  must be less than 2. If the  $N = 0$  or if the  $N = 1$ , (20) can be evaluated simply. We let  $x = \omega\theta$  and substitute in (20). Hence,

$$\tilde{\sigma}(\theta) = \frac{2\pi K}{\omega^{2-N}} \int_0^{x_0} x^{1-N} J_0(x) dx \quad (21)$$

where,  $x_0 = \omega\epsilon$ . For  $N=0$ , we have that, (3)

$$\tilde{\sigma}(\theta)_{N=0} = \frac{2\pi K}{\omega^2} x_0 J_1(x_0) \quad (22)$$

For  $N = 1$ ,

$$\widetilde{\sigma(\theta)}_{N=1} = \frac{2\pi K}{\omega} \int_0^{x_0} J_o(x) dx \quad (23)$$

The integral cannot be expressed in simple form, but because of its importance it has been tabulated <sup>(4)</sup>.

The Schripps data indicates that  $N$  is not an integer or a simple fraction but something between 1.5 and 1.6. Consequently, it is necessary to evaluate (21) for the general case of  $N < 2$ .

To simplify the equation somewhat, we let  $(1-N) = n$  and rewrite (21) as,

$$\widetilde{\sigma(\theta)} = \frac{2\pi K}{\omega^{n+1}} \int_0^{x_0} x^n J_o(x) dx \quad (24)$$

We expand the  $J_o$  into its series representation and integrate term by term, i.e.,

$$\widetilde{\sigma(\theta)} = \frac{2\pi K}{\omega^{n+1}} \left\{ \int_0^{x_0} x^n dx - \frac{1}{2^2} \int_0^{x_0} x^{n+2} dx + \frac{1}{2^2 \cdot 4^2} \int_0^{x_0} x^{n+4} dx \dots \right\} \quad (25)$$

or,

$$\widetilde{\sigma(\theta)} = \frac{2\pi K}{\omega^{n+1}} \left\{ \frac{x_0^{n+1}}{(n+1)} - \frac{1}{2^2} \cdot \frac{x_0^{n+3}}{(n+3)} + \frac{1}{2^2 \cdot 4^2} \cdot \frac{x_0^{n+5}}{(n+5)} - \dots \right\} \quad (26)$$

Taking out  $x_o^{n+1}$  we obtain,

$$\widetilde{\sigma}(\theta) = 2\pi K \left( \frac{x_o}{\omega} \right)^{n+1} \left\{ \frac{1}{(n+1)} - \frac{1}{2^2} \cdot \frac{x_o^2}{(n+3)} + \frac{1}{2^2 \cdot 4^2} \cdot \frac{x_o^4}{(n+5)} - \dots \right\} \quad (27)$$

Substituting back for N, we have,

$$\widetilde{\sigma}(\theta) = 2\pi K \left( \frac{x_o}{\omega} \right)^{(2-N)} \left\{ \frac{1}{(2-N)} - \frac{1}{2^2} \cdot \frac{x_o^2}{(4-N)} + \frac{1}{2^2 \cdot 4^2} \cdot \frac{x_o^4}{(6-N)} - \dots \right\} \quad (28)$$

So that the transform is like  $J_o(x_o)$  with modified coefficients depending on N, the slope of the scattering curve.

In order to complete (28), we evaluate the constant K by considering the integral of (18), i.e.,

$$2\pi \int_0^\epsilon \sigma(\theta) \theta d\theta = 2\pi K \int_0^\epsilon \theta^{1-N} d\theta \quad (29)$$

If we call the integral of  $\sigma$  up to  $\epsilon$ , S, then,

$$K = \frac{S(2-N)}{2\pi \epsilon^{(2-N)}} \quad (30)$$

Substituting back in equation (28) we obtain that,

$$\tilde{\sigma}(\theta) = \frac{(2-N)S}{\epsilon^{(2-N)}} \left( \frac{x_0}{\omega} \right)^{(2-N)} \sum \quad (31)$$

where,  $\sum$  represents the series solution. Since  $\frac{x_0}{\omega} = \frac{\omega\epsilon}{\epsilon} = \epsilon$ , we finally obtain that,

$$\tilde{\sigma}(\theta) = (2-N) S \sum \quad (32)$$

This form of the transform is useful as the value  $s$  has been calculated by the Schripps data. As can be seen when  $N=0$  and  $N=1$ , (32) becomes equations (22) and (23) respectively.

Equation (32) can now be substituted back into the equation for  $\tilde{\sigma}$ , equation (17), and can be written as,

$$\tilde{\sigma}(\omega_\theta) = e^{-\alpha R} \cdot e^{(2-N)S \sum R} \quad (33)$$

Consequently  $\tilde{\sigma}(\omega_\theta)$  depends on  $\alpha$ ,  $N$ ,  $\epsilon$  and  $s$ , the water characteristic and the range  $R$ .

It is instructive to compare this result with the result given by Wells, assuming a mathematical model for  $\sigma(\theta)$ . Wells gives for  $\tilde{\sigma}$ ,

$$\tilde{\sigma}(\omega_0) = e^{-\alpha R} \cdot e^{\frac{s(1 - e^{-\omega\theta_0})R}{\omega\theta_0}}$$

(34)

where,  $\theta_0$  is a characteristic of the scattering function. For  $\omega = 0$ ,  $\tilde{\sigma} = e^{-\alpha R} \cdot e^{sR}$ , whereas equation (33) also gives the same result. As  $\omega$  goes to 0, both expressions give  $\tilde{\sigma} = e^{-\alpha R}$ . However, values in between do not correlate. For example, at  $x_0$  and  $\omega\theta_0 = .5$ , the  $\tilde{\sigma}$  of Wells gives  $e^{-\alpha R} \cdot e^{.79sR}$  whereas equation (33) becomes  $\tilde{\sigma} \approx e^{-\alpha R} \cdot e^{(1 - .06\frac{(2-N)}{(4-N)})sR}$ . The coefficient of  $sR$  becomes .97 for  $N = 0$ , .98 for  $N = 1$  and about .99 for  $N = 1.5$ . As this occurs as an exponential, the two expressions for  $\tilde{\sigma}$  would deviate greatly.

Consequently, the Wells  $\tilde{\sigma}$  is a more rapidly decaying function than equation (33) and is the result of assuming a value for  $\theta = 0$ . Equation (33) represents a more gradually decaying function resulting from a more peaked  $\sigma(\theta)$  for small angles as the experimental data indicates.

### III EVALUATION OF DETECTOR RESPONSE TO AERIAL IMAGE

In section II we have derived a nearly closed form expression for the degradation of a received image due to the sea-water characteristics. In a viewing system, this degraded aerial image must now be recorded by whatever detector is being used in the system. How the detector 'reads' the aerial image will determine the response obtained from the overall system.

The expression that was derived in equation (12) represents the resultant intensity in the aerial image in spatial frequency units. We must now consider what happens as a detector records the image to give the system response. The detector can be any one of several systems used for detection. For example, the detector can be a television camera, a photodiode imaging array, photographic film, image dissector tube or the newly developed charge coupled device. In order to make this analysis very general so that whatever detector is used, the resulting expressions will assess the ability of each type of detector to reproduce the aerial image, for all detectors a recording medium's resolution element can be defined. For TV, it is the electron beam spot size and for photographic film it is the grain size and so on. Due to the finite size of the recording element, the aerial image will be further degraded as for each detector there is a required signal to noise ratio for the element size necessary for detection.

Returning to equation (11) of section II where the received intensity is expressed in angular coordinates of the image plane, we wish to determine the resultant intensity expression in the detector plane. We represent the aerial image intensity as  $I(\theta_x, \theta_y)$  and the detector intensity as  $I(\theta_u, \theta_t)$ . Let the detector spot size

have a radius of  $\theta_s$  which spreads out each point of  $I(\theta_x, \theta_y)$  into a diameter of  $2\theta_s$ . This can be expressed mathematically as the function  $\text{circle}(\theta)/\pi\theta_s^2$  (i.e. a uniform circle which intercepts  $\frac{1}{\pi\theta_s^2}$  fraction of the incoming image. The angular coordinates of the resultant distribution we call  $I(\theta_u, \theta_t)$ . Hence, similar to the object-image relationship used before, we have that,

$$I(\theta_u, \theta_t) = \iint_{\text{Aperture}} I(\theta_x, \theta_y) \frac{\text{circle}(\theta_u - \theta_x, \theta_t - \theta_y)}{\pi\theta_s^2} d\theta_x d\theta_y \quad (35)$$

As this is a convolution of  $I(\theta_x, \theta_y)$  with the recording spot, we transform (35) to yield,

$$I(\omega_{\theta_u}, \omega_{\theta_t}) = I(\omega_{\theta_x}, \omega_{\theta_y}) \cdot \frac{\widetilde{\text{circle}(\theta)}}{\pi\theta_s^2} \quad (36)$$

But the circle ( $\theta$ ) has the transform  $\pi\theta_s^2 2J_1(\omega\theta_s)/\omega\theta_s$ .  
Hence (36) becomes,

$$I(\omega_{\theta_u}, \omega_{\theta_t}) = I(\omega_{\theta_x}, \omega_{\theta_y}) \cdot \frac{2 J_1(\omega\theta_s)}{\omega\theta_s} \quad (37)$$

Equation (37) expresses the additional degradation of the image spectrum due to the finite recording spot size. Due to the manner in

which  $I(\omega_{\theta_x}, \omega_{\theta_y})$  was derived, equation (12),  $I$  represents the total number of photons passed by the system at a given frequency. For example, at  $\omega = 0$ ,  $I(0,0)$  represents the total illumination or total number of photons in the image plane. Consequently, substituting the expression for  $I(\omega_{\theta_x}, \omega_{\theta_y})$ , equation (12) and expressing now the  $I(\omega_{\theta_u}, \omega_{\theta_t})$  in terms of photons, we have that,

$$N(\omega_{\theta_u}, \omega_{\theta_t}) = \frac{n_0 D^2}{4} \tau_{sw} \rho(\omega_{\theta_s}, \omega_{\theta_t}) \frac{2 J_1(\omega \theta_s)}{\omega \theta_s} \quad (38)$$

In order to calculate the resultant signal to noise photon ratio ( $S/N$ ), we consider the effect of background light in the image plane.

The effect of background light can be included by treating the background as a uniform object in object space whose diffuse reflectivity is given by,

$$\rho_B(\theta) = \pi \sigma_B r_{eff} \text{circle}(\theta) \quad (39)$$

where,

$\sigma_B$  = the scattering function value for seawater at  $180^\circ$

$r_{eff}$  = the effective distance through which backscattering occurs

$\text{circle}(\theta)$  = represents a uniform beam used for illuminating the object

It is noted that since  $\sigma_B$  has units of  $1/\text{distance steradian}$ , the

$\pi$  is necessary because of the way  $\rho$  was originally defined. The value of  $r_{eff}$  can be calculated by knowing the size of the illuminating beam, the angle between illuminating beam and viewing system direction

and range R. Provided  $r \ll R$ , it can be shown<sup>(5)</sup> that,

$$r_{\text{eff}} \approx \frac{2 \theta_{\text{MAX}} R}{\tan \gamma} \quad (40)$$

where  $\theta_{\text{MAX}}$  = angular radius of illuminating beam at the object

$\gamma$  = angle between illuminating beam and direction of viewing

The transform of  $\rho_B(\theta)$  is just,

$$\widetilde{\rho}_B = \pi \sigma_B r_{\text{eff}} \widetilde{\text{CIRCLE}}(\theta) \quad (41)$$

or,

$$\widetilde{\rho}_B = \frac{\pi \sigma_B r_{\text{eff}} A_\theta 2 J_1(\omega \theta_{\text{MAX}})}{\omega \theta_{\text{MAX}}} \quad (42)$$

where  $A_\theta$  = angular area of the illuminating beam at the object. Since the background light traverses the same path length as the object reflected light, we can write that,

$$N(\omega_{\theta_u}, \omega_{\theta_t}) = \frac{n_0 D^2}{4} \tau_{sw} \cdot \frac{2 J_1(\omega \theta_s)}{\omega \theta_s} \left\{ \widetilde{\rho}_o + \widetilde{\rho}_B \right\} \quad (43)$$

where,,  $\widetilde{\rho}_o$  = reflectivity spectrum of object

$\widetilde{\rho}_B$  = given by equation (42)

Equation (43) was derived in such a way that  $N$ (i.e.  $N_s + N_B$ ) at  $\omega = 0$  represents the total number of photons (signal + background) available in the entire image plane. This can be seen by considering the meaning of  $N$  when  $\omega = 0$ . From equation (35), the  $I(\theta_u, \theta_t)$  represents the number of photons/steradian as the recording spot explores the image plane with coordinates  $\theta_u, \theta_t$ . The transform of this is defined as,

$$\widetilde{I}(\theta_u, \theta_t) = \iint_{\text{Aperture}} I(\theta_u, \theta_t) e^{-\zeta(\omega_u \theta_u + \omega_t \theta_t)} d\theta_u d\theta_t \quad (44)$$

When  $\omega = 0$ , the transform is just the integration of the  $I(\theta_u, \theta_t)$  over the image plane.

In order to define the S/N photon ratio properly, we recast equation (35) so that  $I(\theta_u, \theta_t)$  represents the total number of photons at the coordinates  $\theta_u, \theta_t$  in the recording plane rather than in terms of photons/unit steradian. This is done by treating the recording spot size as just passing the number of photons contained in the recording spot, i.e.,

$$N(\theta_u, \theta_t) = \iint_{\text{Aperture}} I(\theta_x, \theta_y) \text{circle}(\theta_u - \theta_x, \theta_t - \theta_y) d\theta_x d\theta_y \quad (45)$$

Equation (45) expresses the number of photons and hence current or voltage in the read-out system used at the coordinates  $\theta_u, \theta_t$ . Transforming (45), we have that,

$$\widetilde{N}(\theta_u, \theta_t) = \pi \theta_s^2 \widetilde{I}(\theta_x, \theta_y) \mathcal{Z}_s(\omega_\theta) \quad (46)$$

or,

$$\widetilde{N}(\theta_u, \theta_t) = \frac{\pi \theta_s^2 \widetilde{I}(\theta_x, \theta_y) 2 J_1(\omega \theta_s)}{\omega \theta_s} \quad (47)$$

Equation (47) represents the resultant equivalent number of photons passed by a read-out system. It is noted that it no longer represents the total number of photons in the image plane.

It is known that the arrival probability for photons on a surface is given by Poisson statistics as,

$$P(x; N) = \frac{N^x e^{-N}}{x!} \quad (48)$$

where,  $P(x; N)$  = probability of receiving  $x$  number of photons when  $N$  is the average number. If the detector has a quantum efficiency of  $Q$ , it can be shown that the photoelectron signal to noise ratio is just,<sup>(6)</sup>

$$(S/N)_{\text{photoelectron}} = \sqrt{NQ} \quad (49)$$

Consequently we can write that,

$$(S/N) \cdot (S/N) = N Q \quad (50)$$

In frequency space this becomes,

$$\Phi_{S/N} = Q \tilde{N} \quad (51)$$

where the  $\Phi_{S/N}$  is the autocorrelation of the transform of S/N. The introduction of the autocorrelation of the transform of S/N becomes a more meaningful criterion in terms of the transmission of information by a system than speaking of a S/N at a given point in the image. For example, at  $\omega = 0$ , the  $\Phi_{S/N}$  represents,

$$\Phi_{S/N}(\omega=0) = \langle (S/N)^2 \rangle \quad (52)$$

where the brackets indicate a time or ensemble average. Hence the average of the  $(S/N)^2$  over the entire image plane is just the variance in S/N. The square root of this function would be the standard deviation of S/N over the image plane. For other spatial frequencies a similar interpretation could be given.

From the point of view of eventually developing a recognition system, the ability of the system to transmit frequency information becomes paramount.

In this derivation, we have not attempted to include electronic noise of the read-out system as in general the design of the read-out system is made so that the shot noise is the major source of noise.

#### IV. EFFECT OF DETECTOR SCANNING

In section III, we have derived the expressions that relate the effect of the recording medium's spot size to the resultant response from the detector. We consider now the effect of line scanning on the final image.

Equation (43) was derived on the assumption that the recording spot size explores the image plane continuously in all directions. In the case of line scanning as in a television camera, (43) must be modified to reflect this line scanning. We can treat the scanning system as if the aerial image is sampled, say in the  $\theta_y$  direction. If the separation between each scan line is called  $\theta_y$  (angular units in the y direction), then it can be shown using sampling theory that equation (43) becomes,

$$N = \frac{n_0 D^2}{4} \sum_{n=-N/2}^{N/2} \left( r_{sw} [\tilde{\rho}_o + \tilde{\rho}_B] \cdot \frac{2 J_1(\omega \theta_s)}{\omega \theta_s} \right) \text{evaluated at } \omega_{\theta_x}, (\omega_{\theta_y} - \frac{2\pi n}{\theta_y}) \quad (53)$$

where  $N$  is the number of TV lines. Equation (53) expresses the fact that the image spectrum is reproduced at intervals of  $2\pi n / \theta_y$  in the  $\omega_{\theta_y}$  direction in frequency space. If the highest frequency of the image spectrum to be passed by the system is  $\omega_o$ , then it also can be shown that (53) goes over to (43) when  $\theta_y \leq \pi / \omega_o$ .

The sampling theorem can become important when considering objects with low frequency components which are further degraded by the sea-water transfer function. This will produce a lower frequency limit which allows the use of less scan lines per picture thereby permitting the available information to be passed more rapidly than from continuous scanning (i.e. continuous scanning would not produce add-

itional information about the image).

As an example of how sampling theory permits information retrieval more rapidly, consider the object to be a rectangle (i.e. simulating a cross beam that may be present in an underwater off-shore oil drilling rig). Additionally assume it is covered with barnacles giving a diffuse reflectivity  $\rho$  with an angular width  $\theta_w$  radians and an angular length of  $\theta_L$  radians oriented along the  $\theta_E$  direction, see Figure 1. The reflectivity spectrum of the object becomes,

$$\widehat{\rho}_o = \rho \cdot \theta_L \frac{\sin \frac{\omega \theta_L}{2}}{\omega \theta_L / 2} \cdot \frac{\sin \omega \theta_w / 2}{\omega \theta_w / 2} \cdot \theta_w \quad (54)$$

The highest frequency in the object will be given by the expression,

$$\sin \frac{\omega \theta_w}{2} = 0 \quad (55)$$

or when,

$$\omega_o = \frac{4\pi}{\theta_w} \quad (56)$$

If there were no seawater degradation, then the image should be sampled at  $\theta_y = \pi/\omega_o = \theta_w/4$  to retrieve all the information available about the object. However, because the  $\omega_o$  is multiplied by  $C_{sw}$  in equation (53), the highest frequency is now reduced according to,

$$C_{sw} \sin \omega \theta_w / 2 = 0 \quad (57)$$

This is now governed by the  $\tau_{sw}$  if the limiting value of  $\omega$  due to  $\tau_{sw}$  is less than the  $\omega_o$ . Consequently, depending on the values of  $\alpha$ ,  $s$  nad  $N$  which defines the  $\tau_{sw}$ , the image need only be sampled at  $\theta_y = \pi/\omega(\tau)$ . This value of  $\theta_y$  would be greater than the value computed based on the object limiting frequency. As no new information can be obtained by scanning closer than this, it reduces the number of scan lines necessary per picture or image.

Due to the large number of variables involved in assessing the image quality and subsequent detection (approximately 15), it is necessary to define a scenario of viewing and illumination configuration before the results of this study can be applied. Once the image quality can be assessed then the design on the intelligence required on a robot viewing system can be evolved. See figure 1 for the variables involved before recognition parameters can be designed.

## V. SUMMARY AND RECOMMENDATIONS

During this study, we have established the basic framework for assessing the image quality and subsequent detection for underwater viewing systems. In particular we have derived:

- a) the form of the point spread function in frequency space (the transfer function) of sea-water which utilizes available experimental scattering data.
- b) the form of the imaging equations in water.
- c) the equations governing scattering background that reduces the aerial iamge contrast.
- d) the equations governing the degradation of the aerial image due to the finite size of the resolution element of the recording system.
- e) the frequency space equivalent of the S/N that results from shot noise
- f) the equations governing the line scanning of the aerial image

It is recommended that the next phase of this study should address the following areas:

- a) Establish a viewing system scenario
- b) Assess the ability of the following four photoelectric detectors to transmit image spatial frequencies;
  - 1) conventional TV
  - 2) photodiode array
  - 3) image dissector photomultipier
  - 4) charge coupled device
- c) Develop an optical algorithm tha can recognize preprogrammed image information

- d) Fabricate an optical simulator for sea-water and detector degradation of prescribed images in order to assess the optical algorithms developed.
- e) Design and fabricate an optical recognition module to be used with a developed viewing system.

REFERENCES

- (1) Willard H. Wells, "Optics of the Sea", AGARD Lecture Series No. 61, NATO, AGARD-LS-61, Section 3.3, August 1973.
- (2) Theodore J. Petzold, Contract N62269-71-C-0676, NADC, Warminster, Pa., Scripps Institute of Oceanography, San Diego, Calif., Final Report, Oct. 1972.
- (3) Frank Bowman, "Introduction to Bessel Functions", Dover Publications, New York, New York, 1958.
- (4) Yudell L. Luke, "Integrals of Bessel Functions", McGraw-Hill Book Co., Inc., New York, New York, 1962.
- (5) Harry Sadjian, Contract N00014-77-C-0344, ONR, Bay St. Louis, Miss., General Sensors, Inc., Ft. Washington, Pa., Progress Report # 1, June 1977.
- (6) D.L. Fried, App. Optics, 4, No. 1, Jan. 1965, pg. 79.
- (7) Joseph W. Goodman, "Introduction to Fourier Optics", McGraw-Hill Book Co., Inc., New York, New York, 1968.

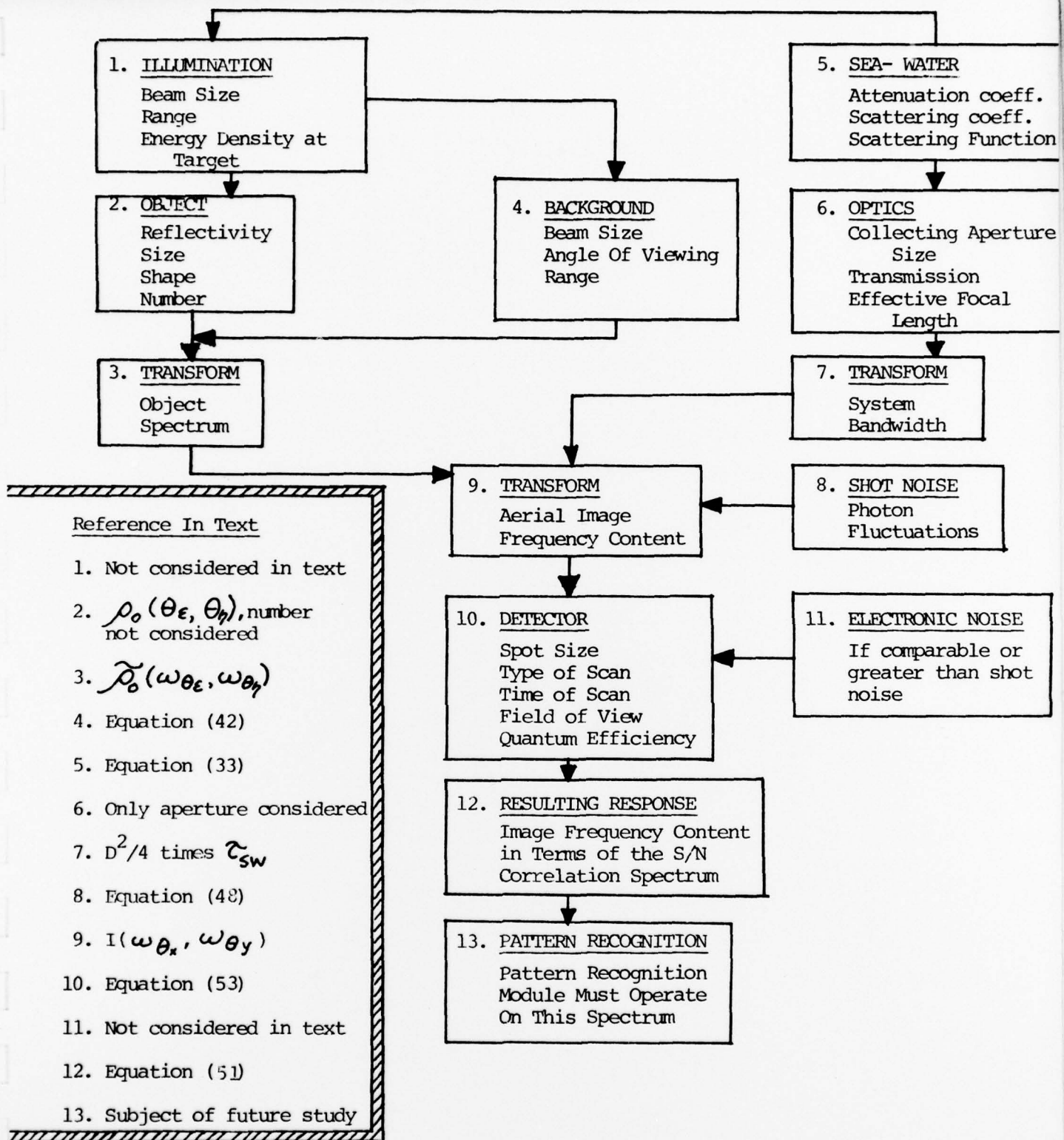


FIGURE 1. Flow Diagram Of The Steps Necessary, With The Variables Involved, To Determine The Image Quality With Subsequent Detector Retrieval In Frequency Space.

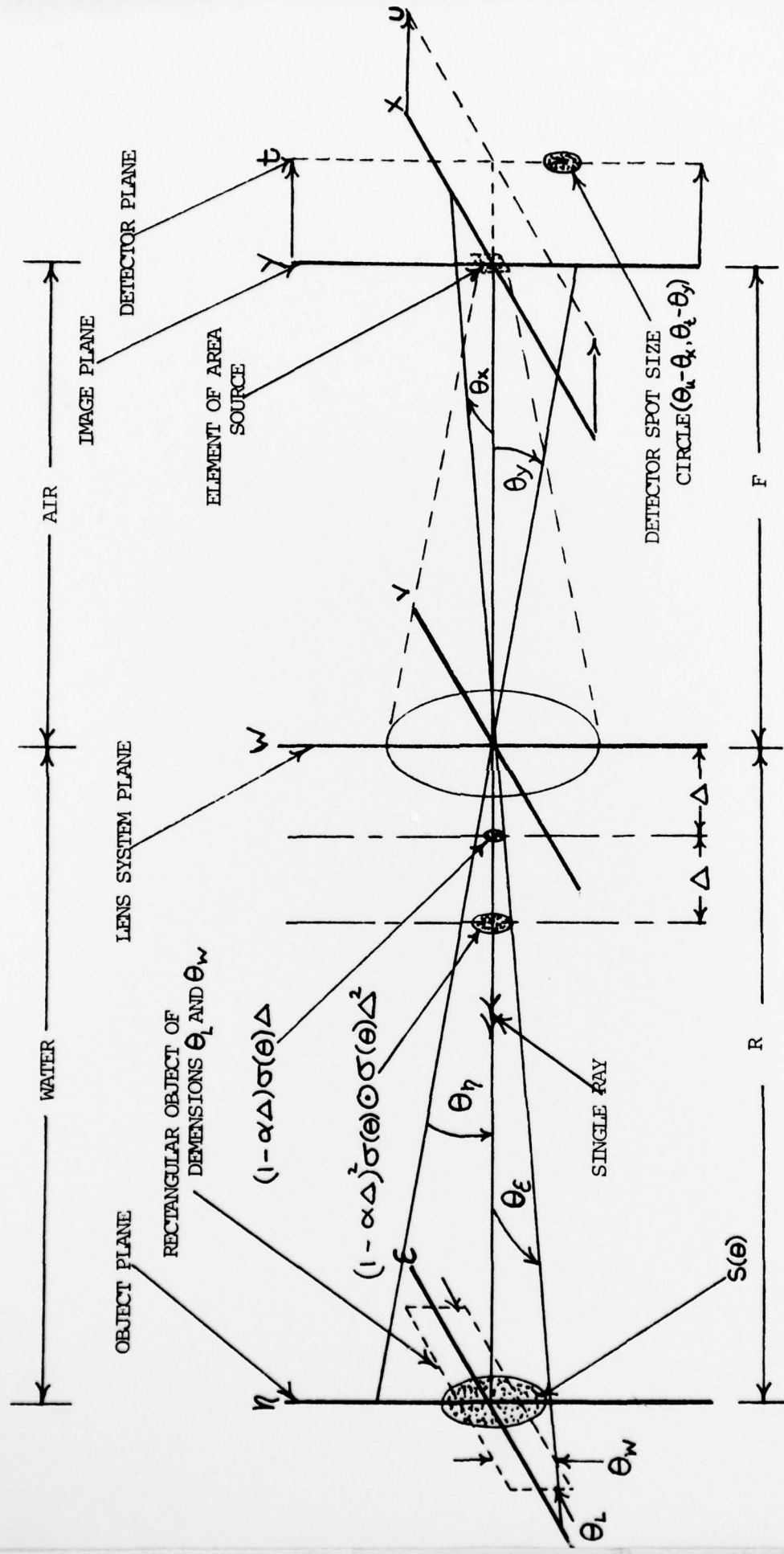


FIGURE 2. Geometry Used To Derive The Imaging Equations In Water With Subsequent Detector Read-out (See Text).

**GENERAL**



**SENSORS, INC.**